ASSESSMENT OF THE HARDNESS AT THE MICROSTRUCTURAL LEVEL IN WELDED CONNECTIONS FORMED USING 316L AND S235 MATERIALS

Gabriela-Victoria MNERIE [1], Horia Florin DAȘCĂU[2], Iuliana DUMA[3], Emilia DOBRIN[4],
[1] National R&D Institute for Welding and Material Testing, ISIM Timisoara, Romania, gmnerie@isim.ro
[2] National R&D Institute for Welding and Material Testing, ISIM Timisoara, Romania, hdascau@isim.ro
[3] National R&D Institute for Welding and Material Testing, ISIM Timisoara, Romania, iduma@isim.ro
[4] National R&D Institute for Welding and Material Testing, ISIM Timisoara, Romania, edobrin@isim.ro

ABSTRACT: The growing adoption of stainless steel primarily results from increased requirements concerning the resistance to corrosion in the applications and structures where they are used. The primary characteristic of austenitic steels lies in their ability to form a protective oxide layer on their surface, bolstering their resistance to oxidation. Within the category of corrosion-resistant steel types, austenitic steel stands out because of its robust mechanical properties. These steels are readily deformable, resistant to wear and, if needed, abrasive damage. Nonetheless, they are also susceptible to stress-corrosion cracking, intracrystalline corrosion, and pitting corrosion. This investigation explores the results that unveil distinct dissimilar samples of the half V joint. These samples were employed to scrutinize the heat-affected zones, both in the S235 and the 316L steel. Furthermore, the welded connections exhibited elevated hardness values when repairs were performed without access to all the previous information about their fabrication. After flux-cored arc welding, the S235 retains its original structure, while the 316L steel maintains its austenitic structure with sporadic bands of ferrite σ and chromium carbides.

KEYWORDS: microstructure, hardness evaluation, 316L, S235, corrosion resistance

1. INTRODUCTION

Welding dissimilar metals is a common practice across various industries, and the performance of these welded joints is often critical for the proper functioning of the assembled parts. The mechanical strength of these welds enables the design of lighter and more compact structures, reducing the need for extensive manufacturing processes.

An essential phenomenon in this context is spinodal demixing, a thermodynamic mechanism wherein a single phase autonomously splits into two separate phases without necessitating nucleation [1]. This phase demixing transpires in the absence of any thermodynamic obstacles. Unlike conventional phase separations driven by thermodynamic fluctuations, spinodal demixing does not entail such nucleation occurrences [2].

During spinodal demixing, the δ-ferrite phase, known as the α phase, and rich in iron, segregates to generate a phase enriched in chromium. While spinodal decomposition is not easily noticeable in materials aged for shorter durations or at temperatures below 400°C, it becomes more pronounced with longer aging times, reaching thousands of hours or during repairs involving high heat input.

Moreover, after the repair procedure, the phase precipitates grow considerably larger than the initial sinusoidal composition profile. This phase demixing and the subsequent formation of the fragile α phase contribute to the embrittlement of the welded joint. Consequently, welds made of 316L stainless steel display heightened hardness, yield strength, and tensile strength [3].

This embrittlement, induced by the formation of the α phase following spinodal decomposition, also enhances vulnerability to stress corrosion cracking and intracrystalline cracking. The Vickers hardness examination entails pressing a square-based pyramidal diamond indenter into the surface of the specimen using a predetermined force. After indenter removal, the diagonals of the resulting impression are gauged, and the hardness value, represented as HV for Vickers testing, is computed.

To assess the hardness of a welded joint and its adjacent regions, hardness maps are created by conducting Vickers hardness tests incrementally across the weld, the Heat Affected Zone (HAZ), and the base material region. The test locations are spaced apart at a distance that is at least three times the diagonal measurement of the indentation. The results are then presented both in tabular and graphical formats. This approach allows for a comprehensive examination of hardness changes throughout the welds entire surface, avoiding interference between data points due to work hardening and plastic deformation [4].

2. MATERIALS AND METHODS

2.1 Materials used

316L austenitic stainless steel is a blend comprising iron, chromium, nickel, and molybdenum. Chromium has a vital function in augmenting the corrosion resistance of this mixture. However, it can also participate in the development of a debilitating stage when spinodal demixing takes place in the steel. On the contrary, nickel promotes the generation of the austenitic phase. Molybdenum serves to stabilize the ferrite and boost the alloy's strength at elevated temperatures [5].

Applications for 316L stainless steel include biomedical implants, chemical processing, food processing, photography, pharmaceuticals, textile finishing, and marine exterior trim. Table 1 displays the chemical composition of 316L stainless steel.

Table 1. Composition of the base materials from a chemical standpoint (wt%), [5]

Specification	*Fe*	*C*	*Cr*	*Cu*	*Mn*	*Mo*	*Ni*	*P*	*S*	*Si*
316L	Bal.	≤0.03	≤18.50	≤0.26	≤2.00	≤2.50	≤13.00	≤0.035	≤0.035	≤1.00

316L, also known as Grade 1.4404, is an austenitic stainless steel of the AISI 316 family. Its excellent corrosion resistance results from the high chromium and molybdenum levels, coupled with low carbon content. In its hardened state, it exhibits a strength of approximately 600 MPa for larger diameters, but this strength can be enhanced through cold working in smaller sections.

Table 2 displays the specified minimum mechanical properties for annealed type 316L austenitic stainless steel plates, sheets, and strips as required by both ASTM A240 and ASME SA-240 specifications, [6].

Table 2. Mechanical properties of 316L, [6], [7]

Properties	*Value*
Tensile Strength, (min.)	485 MPa
0.2% Yield Strength, (min.)	170 MPa
Elongation at fracture in 50 mm, (min.)	40 %
Reduction of Area, (min.)	50 %
Hardness Brinell (HB), (min.)	190
Hardness, Rockwell (HRB), (min.)	91
Hardness, Vickers (HV), (min.)	199
Charpy Impact, (min.)	103 J

The table 3 presents the physical properties of 316L austenitic stainless steel, including density, melting point, specific heat, electrical resistivity, elastic modulus (modulus of elasticity), thermal conductivity, and more.

S235 steel is a weld-friendly, low carbon manganese steel that boasts good impact resistance, even in sub-zero temperatures.

Table 3. Physical properties of 316L, [7]

Properties	*Value*
Thermal conductivity (W/m·K)	14.0-15.9
Magnetic permeability	≈ 1.01
Electrical resistivity (μΩ·m at 20 °C)	0.74
Density (g/cm^3)	8.0
Specific heat capacity	500 J/kg·K at 20 °C
Melting point	1375-1400 °C
Modulus of elasticity	193 GPa

Typically, this material is provided in its untreated or normalized state, and it comes in multiple versions, identified by extra letters and/or numbers, which introduce minor adjustments to its chemical composition and mechanical characteristics. The machinability of S235 steel is akin to that of mild steel.

Standard applications for S235 carbon steel include construction, engineering, machinery (yellow goods), and tank manufacturing [8].

The chemical composition of carbon steel holds significant importance and is subject to strict regulations. This fundamental factor plays a key role in determining the material's mechanical properties. Table 4 displays the maximum percentage levels of specific regulated elements found in the European structural steel grade S235.

Table 4. Chemical composition of S235 carbon steel (wt%), [8]

Specification	*C*	*Cr*	*Cu*	*Mn*	*N*	*Ni*	*P*	*S*	*Si*
S235	≤0.22	≤0.30	≤0.30	≤0.60	≤0.012	≤0.30	≤0.04	≤0.04	≤0.05

The chemical composition stands as the primary determinant in establishing mechanical properties. A structural steel's mechanical properties provide valuable insights into its suitability for a particular application. These mechanical properties, as outlined in Table 5, encompass attributes like toughness, hardness, and stiffness. However, among these, the most crucial mechanical properties are tensile and yield strength. The nomenclature of these steels is often based on their yield strength, [9].

Table 5. Mechanical properties of S235, [9], [10], [11]

Properties	*Value*
Tensile Strength, (min.)	485 MPa
0.2% Yield Strength, (min.)	170 MPa
Elongation at fracture in 50 mm, (min.)	40 %
Reduction of Area, (min.)	50 %

Hardness Brinell (HB), (min.)	190
Hardness, Rockwell (HRB), (min.)	91
Hardness, Vickers (HV), (min.)	199
Charpy Impact, (min.)	103 J

S235 carbon steel exhibits outstanding physical properties, rendering it suitable for diverse applications. With a density of 7.85 g/cm³ and a melting point ranging from 1430 to 1490°C, it offers excellent material characteristics. Notably, its thermal conductivity is 52 W/mK, making it ideal for applications involving heat transfer. Additionally, S235 steel boasts a specific heat capacity of 490 J/kg/K, signifying its ability to absorb significant heat while keeping its temperature stable [12].

2.2 Equipments used

The metallographic grinding and polishing machine (figure 1) is from the FORCIPOL 102 series. As a laboratory equipment, it features a single wheel, variable rotation speeds, and a digital display, allowing for the adjustment of the optimal speed for each individual preparation process. It is the best choice for laboratories that prepare a wide range of different materials, from very small to very large components.

This is a grinding and polishing machine with a 200-300 mm wheel diameter, a standard Forcipol control unit interface, variable speed between 50-600 rpm, with the option of wheel rotation in both clockwise and counterclockwise directions, digital display, a 1.0 HP motor with overload protection.

The technical specifications of Forcipol 102 are presented in Table 6.

Table 6. Forcipol 102 technical data, [13]

Number of weels	1
Wheel diameter	Ø 200 – 300 mm
Wheel speed	50-600 rpm
Wheel rotation direction	CW / CCW
Base motor power	1 HP
Dimension, W x D x H	450 x 740 x 340 mm
Weight	50 kg

The macroscopic examination was performed using the Carl Zeiss Jena optical microscope, and Vickers HV10 hardness tests were carried out with the Zwick 3212 equipment (figure 2), in ambient atmosphere. The hardness testing system consists of the base unit, accessories, and the optical measurement system. It is widely used in testing modern mechanical and technological materials. Material hardness provides an excellent indication of the mechanical properties of a material.

Technical specifications:

- Testing load range: 0.2 - 30 kg;
- Vickers scales: HV0.2 / HV0.3 / HV0.5 / HV1 / HV2 / HV3 / HV5 / HV10 / HV20 and HV30;
- 136° Vickers diamond indenter;
- 20x + 40x magnification objective.

Figure 1. Forcipol 102, Modular metallographic grinding and polishing machine

Figure 2. Zwick 3212 Hardness equipment

3. RESULTS AND DISCUSSION

The samples analysed are part of a new experiment involving a solution with detachable links for eccentrically braced frames with recentring capacity, as depicted in Figure 3. The indentation's precise location was ascertained through a metallographic inspection. Figure 3 delineates the customary zones for positioning individual indentations. Series 1 to 3 and 13-15 provide insights into the unaffected base metal, while series 4-6 and 10-12 correspond to the Heat-Affected Zone (HAZ), and series 7 to 9 relate to the weld metal.

To mitigate the impact of distortion caused by the indentation, a minimum separation distance of at least

2.5 times the average diagonal or diameter of the nearest adjacent indentation point was maintained from the central point of each individual indentation in all directions.

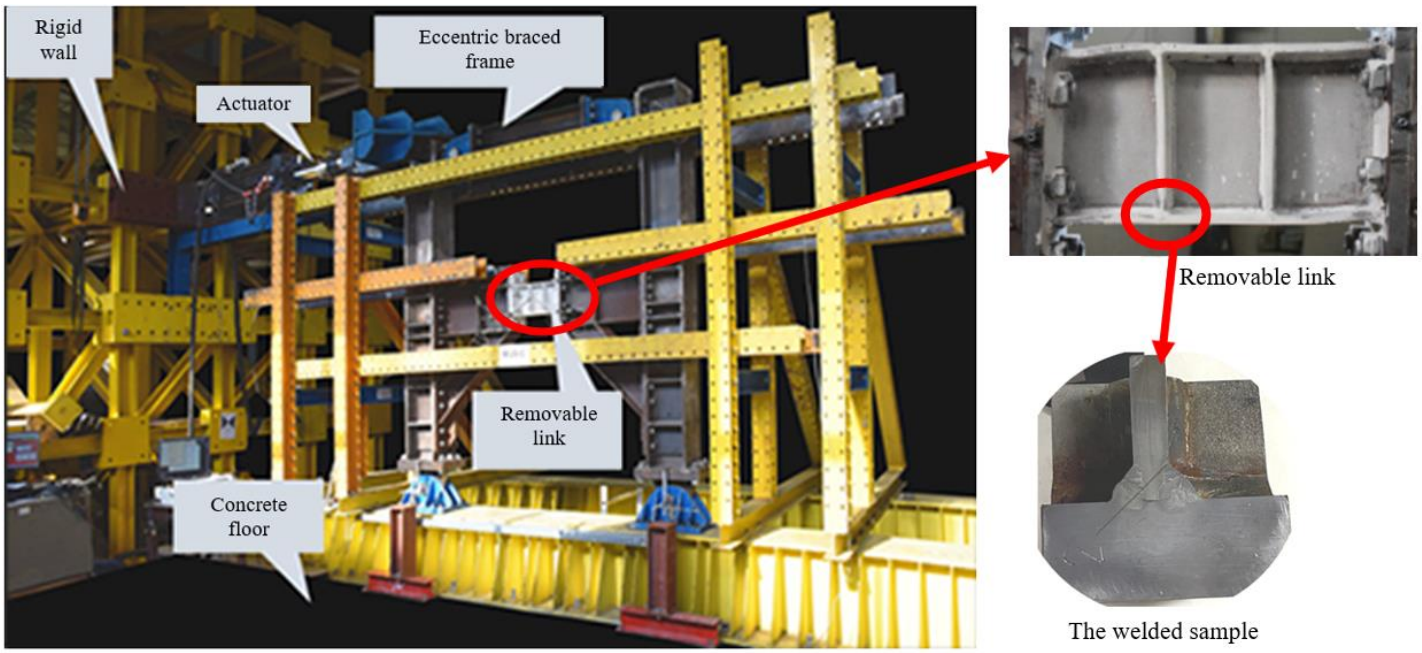

Figure 3. The experimental setup for isolated link tests, [14], [15], [16]

After the completion of the polishing procedure, carbon and austenitic steel specimens underwent etching using a Nital solution, prepared by dissolving 1-5 ml of nitric acid in 95-99 ml of ethyl alcohol for non-alloyed and low-alloyed steel. In the case of stainless steel samples, a blend of hydrochloric acid and nitric acid was utilized, comprising 39 ml of water, 52 ml of hydrochloric acid, and the addition of 50 g of ferric chloride.

The reagent was stirred until the ferric chloride was fully dissolved. The surface of each polished weld sample was immersed at 30-second intervals until the weld became discernible on the polished surface. Figure 4 displays the polished and etched weld.

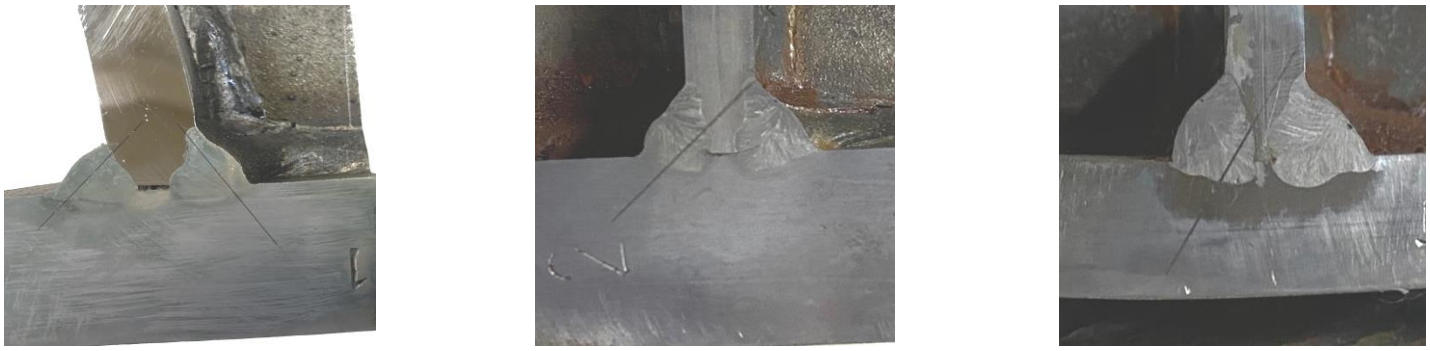

a) b) c)

Figure 4. The welded samples that have been prepared metallographically (left side of the sample)
a) Face 1, b) Face 2, c) Face 3

The Vickers hardness measurements (table 7 and figure 5 - a, b, c) in the Heat-Affected Zone (HAZ) exhibited slight increases compared to those in the weld and the base metal. This slight variation can be attributed to the fact that the temperature fluctuations during the welding process did not significantly alter the phase composition and structure of 316L steel. The HAZ region extended approximately 1 to 1.5 mm in width on both sides of the three specified areas.

Table 7. Chemical composition of S235 carbon steel (wt%), [8]

SH-2DS-C	*BM up*	*HAZ up*	*Weld*	*HAZ down*	*BM shoulder*
Face 1 - Left	210	411	379	384	235
	229	394	375	388	229
	257	383	384	405	232
Face 2 - Left	222	377	359	388	241
	239	381	374	382	232

	244	371	388	391	229
Face 3 - Left	224	385	360	364	244
	226	389	372	370	241
	239	381	368	381	243

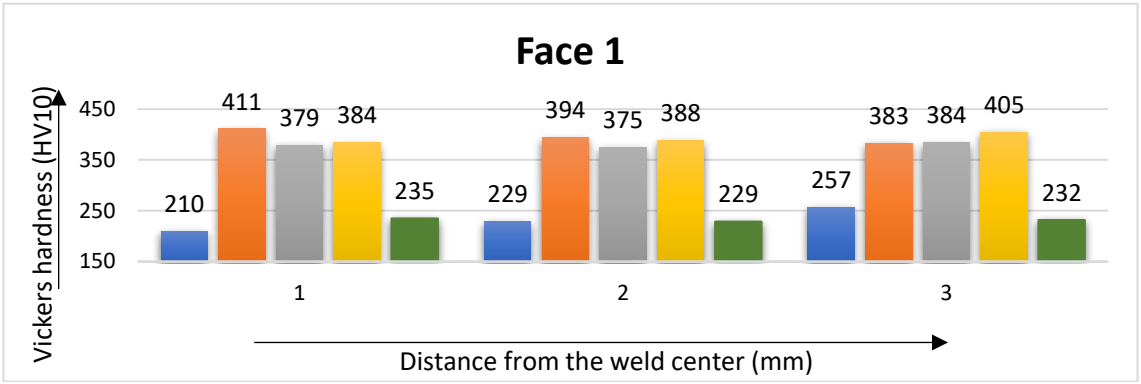

(a)

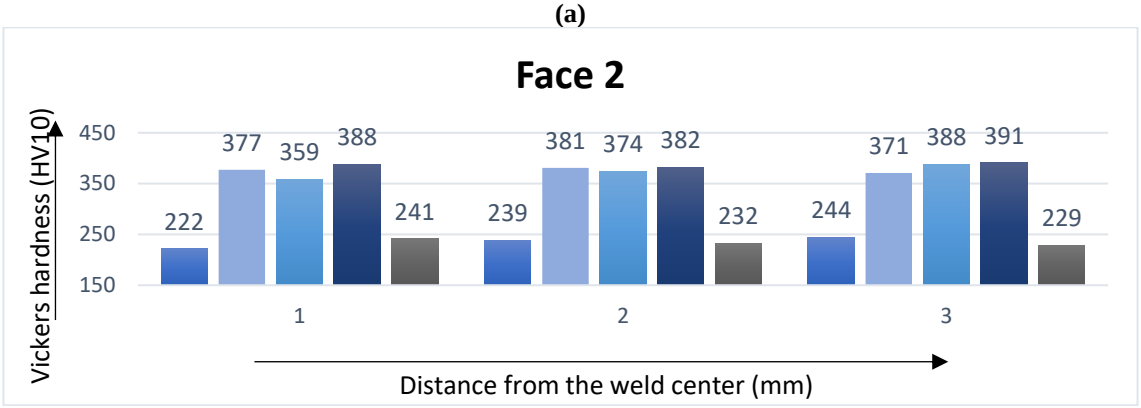

(b)

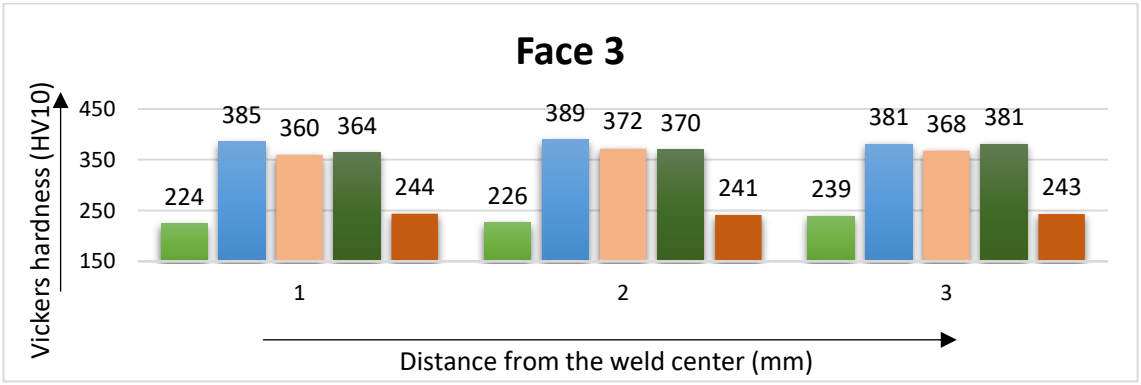

(c)

Figure 5. Vickers hardness measurements in weld areas
a) Face 1, b) Face 2, c) Face 3

Vickers hardness assessments using a 10 kgf/mm² load were executed in accordance with ISO 9015-1. Hardness assessments were carried out at the weld, the heat-affected zone, and the base material to gauge the spectrum of hardness readings within the welded connection. Upon scrutinizing the hardness readings and connecting them to the established hardness values of the base and filler materials, it became apparent that the results did not conform to the required hardness test criteria as outlined in SR EN ISO 15614-1, which dictates a maximum value of 380 HV 10. However, a complication arises from the fact that the stainless steel used in this case falls under the group 8.1 classification of SR ISO/TR 15608, a material category that lacks specified hardness values due to a deficiency in statistical data in comparison to other materials. In this material, it is believed that hardening occurs through the precipitation of chromium carbides. This phenomenon was exacerbated by the presence of a percentage of non-alloyed steel in the molten metal, further promoting the formation of chromium carbides and ultimately resulting in increased brittleness.

4. CONCLUSIONS

The specimens extracted from the links have verified the existence of corner welds in lieu of the ones originally designated at the intended depth in the project. In contrast to the 316L base metal, the weld

contains a greater amount of carbon. This is noticeable through the elevated hardness values and leads to the precipitation of chromium carbides. The δ-ferrite phase concentration in the weld exceeds the optimal thresholds needed to inhibit the creation of a network of chromium carbides. Consequently, alternative methods need to be considered to address this concern. A sequence of HV10 Vickers hardness tests was carried out on portions of the weld, the thermally affected regions, and the underlying material. It was noted that, alongside the described occurrences, there existed to some degree an alternative cracking mechanism typical of austenitic stainless steels and heat-resistant steels. This mechanism resulted from reheat cracking, commonly referred to as stress relief cracking. The results of the hardness analysis have revealed a phenomenon of increased hardness in the crystalline structure of the welds, attributed to the formation of chromium carbides. This phenomenon was facilitated by the presence of a proportion of base material (non-alloyed steel) in the molten pool, intensifying the oxidation process within the welded joint, resulting in increased brittleness. The precipitation of chromium carbides was expedited during the welding repair procedure, due to the additional heat input, promoting their formation at the grain boundaries. The deposition of chromium carbides along these grain boundaries causes the chromium content to dip below 10.5%, rendering the steel susceptible to oxidation. This, in turn, may lead to the emergence of intergranular corrosion. The obtained hardness values clearly indicate that welding repairs on the links are not advisable. This strategy will serve to minimize the presence of residual stresses within the welded joint while enhancing its strength characteristics. Additional investigations will delve into a more comprehensive examination of hardness in structures fabricated using 316 L stainless steel and various alternative base materials.

5. ACKNOWLEDGEMENTS

The paper was developed under the project number PN-III-P2-2.1-PED-2019-5427, provided by the Ministry of Education and Research of Romania (MEC) through the „Experimental Demonstrative Project" (PED) program, carried out as part of the National Research, Development, and Innovation Plan for the period 2015 - 2020 (PNCDI III), and coordinated by the UEFISCDI.

6. REFERENCES

1. K. Binder, *Theory of first-order phase transitions*, Reports on Progress in Physics, Volume 50, Number 7, doi:10.1088/0034-4885/50/7/001, ISSN 0034-4885, (1987), 783–859.
2. *Dissimilar Metal Welding*, Welding of Metallic Materials, (2023).
3. L.J. Ayers, *The hardening of type 316L stainless steel welds with thermal aging*, Thesis document, Massachusetts Institute of Technology, pp. 783-859, (2012).
4. J. Gorka, S. Stano, *Microstructure and Properties of Hybrid Laser Arc Welded Joints (Laser Beam-MAG) in Thermo-Mechanical Control Processed S700MC Steel*, MDPI, Metals, Volume 8, Number 2, https://doi.org/10.3390/met8020132, 132, (2018).
5. *316 Stainless Steel (AMS 5524/5507)* https://www.matweb.com/search/datasheet.aspx?MatGUID=c02b8c0ae42e459a872553e0ebfab648.
6. *AISI 316L Stainless Steel Properties: Composition, Tensile Yield Strength*, https://www.theworldmaterial.com/aisi-316l-stainless-steel.
7. *AISI Type 316L Stainless Steel, annealed and cold drawn bar*, https://www.upmet.com/sites/default/files/datasheets/316-316l.pdf.
8. *S235 - Structural Steel / Steel Plate*. https://www.murraysteelproducts.com/products/s235-low-carbon-manganese-steel.
9. *Structural Steel - S235, S275, S355 Chemical Composition, Mechanical Properties and Common Applications*, https://www.azom.com/article.aspx?ArticleID=6022
10. *Non-alloy structural steels*, https://www.esb-group.com/en/products-din-en/structural-grade-carbon-steel.
11. *Structural Steels S235, S275, S355, S420 and Their Properties*, https://fractory.com/structural-steels-s235-s275-s355-s420-and-their-properties.
12. *Ovako S235 EN10025-2 (ref) Steel, +AR*, https://www.matweb.com/search/datasheet.aspx?matguid=ffc482278e2e4dc780572160dcada3d1.
13. *Operation & instruction manual, Modular grinding and polishing system*, Forcipol series, Metcon Instruments Ink.
14. *Proiect: Linkuri demontabile hibride din oțel inoxidabil și oțel de înaltă rezistență (HYLINK),* https://www.ct.upt.ro/centre/cemsig/hylink.html.
15. *Raport științific și tehnic 1 și 2, Linkuri demontabile hibride din oțel inoxidabil și oțel de înaltă rezistență (HYLINK)*, https://www.ct.upt.ro/centre/cemsig/hylink_files/HYLINK_RST_1-2_2021.pdf.
16. *Raport științific și tehnic 3, Linkuri demontabile hibride din oțel inoxidabil și oțel de înaltă rezistență (HYLINK)*,

https://www.ct.upt.ro/centre/cemsig/hylink_files/
HYLINK_RST_3_2022.pdf